RC22921 (W0309-170) September 26, 2003
Materials Science

IBM Research Report

The Physical Properties of Cubic PE-ALD TaN Films as Ultra-Thin Cu Diffusion Barrier

H. Kim, C. Lavoie, M. Copel, V. Narayanan, S. M. Rossnagel
IBM Research Division
Thomas J. Watson Research Center
P.O. Box 218
Yorktown Heights, NY 10598

Research Division
Almaden - Austin - Beijing - Haifa - India - T. J. Watson - Tokyo - Zurich

The physical properties of cubic PE-ALD TaN films as ultra-thin Cu diffusion barrier

H. Kim, C. Lavoie, M. Copel, V. Narayanan, and S.M. Rossnagel
IBM T.J. Watson Research Center, Yorktown Heights, NY 10598

Abstract

The plasma-enhanced atomic layer deposition (PE-ALD) is a promising technique to produce high quality metal and nitride thin films at low growth temperature. In this study, very thin low resistivity cubic TaN Cu diffusion barrier (< 10 nm) were deposited by PE-ALD from $TaCl_5$ and hydrogen and nitrogen plasma. The physical properties of TaN thin films including microstructure, conformality, roughness, and thermal stability were investigated by various analysis techniques including medium energy ion scattering, transmission electron microscopy, and atomic force microscopy. Especially, the Cu diffusion barrier properties of PE-ALD TaN thin films were studied by *in situ* analysis technique including synchrotron X-ray diffraction, optical scattering, and sheet resistance measurements during thermal annealing of the test structures. The failure temperatures of PE-ALD TaN films were comparable to those of PVD counterpart. The film structures and diffusion barrier failure mechanisms are discussed.

I. Introduction

TaN has been one of the most widely studied materials as a diffusion barrier for Cu interconnect technology, due to high thermal stability and good adhesion to dielectrics besides the good diffusion barrier property.[1-3] The most popular scheme of diffusion barrier is composed of Ta/TaN bilayer, currently produced by physical vapor deposition (PVD). However, with the scaling down of semiconductor devices, the thickness of diffusion barrier should be less than 5 nm for 45 nm line width and beyond.[4] Thus, the implementation of a thin film deposition technique to produce very thin, high quality diffusion barrier with excellent conformability is imminent. For this purpose, the atomic layer deposition (ALD) is a promising thin film deposition technique, mainly due to the excellent conformality of the deposited film with additional benefits.

The ALD of TaN has been studied for several years now, but there are several technical difficulties to be overcome, including the limited availability of good metal precursor. There are only several available precursors to be used for ALD of TaN; halide precursors including $TaCl_5$, $TaBr_5$, and TaI_5, and metal organic (MO) precursors including pentakis(dimethylamino)Ta (PDMAT), pentakis(diethylamino)Ta (PDEAT), and tert-butylimidotris(diethylamido)tantalum (TBTDET). The only reported method to deposit Ta by ALD was from $TaCl_5$ and hydrogen plasma by current authors.[5] Since all currently available MO precursors contain nitrogen in them, it precludes the deposition of Ta metal films from these precursors. Additionally, the use of MO precursors produce films with high carbon content with low film density.[6] Thus, the use of halide precursor and plasma enhancement to produce TaN films have great benefits.

TaN has various phases as a function of nitrogen content and the microstructure and other properties such as resistivity are dependent upon the nitrogen content.[7,8] Among them, cubic

TaN with N/Ta close to 1 is desirable material for diffusion barrier with good thermal stability and low resistivity. However, the Cu diffusion barrier properties of low resistivity cubic TaN CVD or ALD has been seldom reported, since it is usually difficult to grow this phase by either technique. For example, the thermal CVD from $TaBr_5$ and NH_3 only produced nitrogen rich amorphous TaN_x (x = 1.83) at 425 °C.[9] Later, TaN by MO CVD from PDEAT with different NH_3 flow also produced N rich films with N/Ta > 1.7 at around 300 – 375 °C of growth temperature, although the XRD indicated the existence of cubic TaN phase.[10] The ALD of low resistivity cubic TaN has been rarely successful. The ALD of TaN from $TaCl_5$ and NH_3 has produced high resistivity Ta_3N_5 films, and the use of hydrazine as reducing agent produced similar results.[11] Low resistivity cubic TaN films (as low as 1500 μΩcm) were obtained by using additional reducing agent such as Zn, trimethylaluminum (TMA), or amines, but usually with high impurity incorporation.[11-14]

Previously, we have reported the deposition of low resistivity (350 μΩcm) cubic TaN films by plasma-enhanced ALD (PE-ALD) using $TaCl_5$ and the mixture of nitrogen and hydrogen plasma.[15] We successfully deposited low resistivity cubic TaN films with the controllability of nitrogen content and low Cl content (below 1 at.%) at low growth temperatures below 300 °C. The additional benefit of this approach is the possibility of depositing Ta/TaN bilayer simply by switching nitrogen flow on and off during deposition. In this report, we performed the detailed analysis of low resistivity cubic TaN films by PE-ALD using various analysis techniques including medium energy ion scattering (MEIS), transmission electron microscopy (TEM), and atomic force microscope (AFM) to obtain the physical properties which are important for Cu diffusion barrier applications, including microstructure, surface smoothness, conformality, and chemical composition. The diffusion barrier failure temperature was obtained

by *in situ* measurements using synchrotron X-ray diffraction (XRD), sheet resistance, and optical scattering as a function of film thickness. We focused on the diffusion barrier properties of low resistivity cubic TaN film, especially below 10 nm thicknesses, since with the scaling down of devices the diffusion barrier property of ultra thin layer is important. So far, most of the reports on Ta or TaN diffusion barrier properties have been for films with rather large thickness over 10 nm.[9,10,11,16-23] From the comparative study with PVD TaN as well as ALD and PVD Ta, the diffusion barrier properties and failure mechanisms were discussed.

II. Experimental Procedures

The detailed description of the ALD system is given in previous reports.[15] Sample sizes as large as 200 mm diameter can be loaded and the chamber is pumped by a reactive-gas grade turbo molecular pump with a working base pressure of 10^{-7} Torr. The sample heating was done using a resistive heating plate, providing growth temperatures up to 400 °C. The temperature was read by thermocouple attached to the heater, and calibrated against the thermocouple attached to the sample. Although good quality ALD TaN films are obtained over a wide range of growth temperatures between 200 – 400 °C, the growth temperature was set as 300 °C for these experiments. Additionally, an ultra-high vacuum (UHV) magnetron sputtering chamber is connected through the load lock chamber, and Cu capping layer was deposited on top of TaN ALD films without air exposure for diffusion barrier measurements.

The solid $TaCl_5$ (powder) source contained in a glass tube was used as metal precursor. The glass tube was maintained at 100 °C to develop adequate vapor pressure and all the delivery lines were heated between 130-150 °C to prohibit condensation of the precursor. To improve the delivery, Ar was used as carrier gas and the flow was controlled by a leak valve upstream from

the source tube. Atomic hydrogen and activated N_2 are generated by a quartz tube connected to the sample chamber via a gate valve and hydrogen and nitrogen gases are supplied via a leak valve. The quartz tube is wrapped with a multiple-turn coil set at 13.56 MHz with a power level up to 1200 W. In the current experiment, the gate valve is used between the sample chamber and the tube region such that the precursor is not exposed to the tube region.

The deposition cycle consists of the following steps: exposing the substrate to $TaCl_5$ carried by Ar gas for time t_{TaCl_5}, evacuating the chamber, opening the hydrogen and nitrogen source valves and initiating the RF plasma for a set time t_{exp}, and shutting off the hydrogen and nitrogen source and plasma, allowing the chamber to return to base pressure. Before the cycle begins, the partial pressure of hydrogen and nitrogen were set using leak valves. This cycle ideally results in the complete reaction of the adsorbed $TaCl_5$ layer, and the deposition of a fraction of a monolayer of TaN. For this experiments, t_{TaCl_5} = 2 s, t_{exp} = 5 s, and the total time/cycle = 12 s. Based upon the previous reports,[15] the partial pressure ratio between nitrogen and hydrogen has been set as 0.025, producing stoichiometric cubic phase TaN.

PE-ALD TaN films were grown on Si(001) or on SiO_2 substrates. While Si(001) substrates were dipped to the HF-solution, no further cleaning has been performed on SiO_2 substrates. The film composition has been routinely analyzed by Rutherford backscattering (RBS), and X-ray diffraction (XRD) was used to check the cubic phase of the grown films. The microstructure of the film was analyzed by cross-sectional TEM. The samples were prepared using standard "sandwich" techniques followed by dimpling and ion milling until electron transparency. Structural analysis of the TaN on SiO_2 layers was performed using a JEOL JEM-4000EX microscope operating at 400 kV. In addition, the samples were analyzed with MEIS for the surface sensitive compositional analysis and annealing study for thermal stability. MEIS

results were acquired using 100 keV H^+ ions with normal incidence and 20 degree exit angle (110 degree scattering).

For Cu diffusion barrier measurements, a 200 nm PVD Cu layer was deposited on top ALD TaN, without breaking vacuum, using a power level of 1 kW (dc) in the UHV sputtering system. The pressure during the Cu deposition was 5 mTorr. For comparison, bimetal stacks of Cu/TaN on identical substrates were deposited in a separate UHV sputtering system. The TaN films described above were deposited on HF-dipped polycrystalline Si substrates. A SiO_2 buffer layer placed between the poly-Si and Si (100) was used to electrically isolate the Si(100) substrate during the sheet resistance analysis. Copper diffusion barrier failure was studied using three different *in situ* techniques, including synchrotron XRD, optical scattering, and sheet resistance measurements, conducted simultaneously, while the samples were annealed at a temperature ramp rate of 3 °C/s from 100 to 1000 °C in He environment. The analysis was completed at the National Synchrotron Light Source, Brookhaven National Laboratory on beamline X20C. The detailed description of the analysis technique can be found at the previous reports.[24]

III. Experimental Results

The parametric study has shown that the PE-ALD TaN thin films with stoichiometric composition is grown at P_{N_2}/P_{H_2} = 0.025-0.035.[15] At 300 °C of growth temperature, the Cl content of the film is lower than 1 at.% with low resistivity of 350 μΩcm. The growth rate of the PE-ALD at the given condition was 0.24 Å/cycle with density of 9.8 g/cm^3. Fig. 1a shows the cross sectional TEM image of cubic TaN films deposited on 50 Å thick SiO_2 substrate. XRD of the deposited film have shown that the film is composed of cubic TaN phase, whose intensity

ratio between 111 and 200 peaks depends on growth temperature.[15] It is clearly seen that the film is composed of polycrystalline grains with about 5-10 nm diameter. Overall, the film has dense structure, similar to the ALD TiN reported previously.[25] Since the density of the film is lower than bulk value, the physical thickness observed by TEM is larger than that obtained from RBS results. The crystallinity of the grown films is more evident from the HR-TEM image of the same sample (Fig 1b). The image shows that the film is completely polycrystalline, from the beginning of deposition. This is contrast to the PE-ALD Ta film, which is amorphous at the similar deposition temperature.[5] The interface between TaN and SiO_2 was quite smooth and the d-spacing measurement from the image has confirmed that the grains are composed of cubic TaN. Although Fig. 1 shows the results on thin SiO_2 layer, polycrystalline cubic TaN has also been confirmed on Si substrates.

These results indicate that the deposited PE-ALD TaN film is polycrystalline, with quite smooth surfaces. Similarly, previous report on PE-CVD of TaN from $TaBr_5$ and NH_3 produced cubic TaN at 350 °C, which has very similar XRD pattern from ours.[26] Without plasma activation, the halide precursor reacted with NH_3 produced high resistivity films, with amorphous structure at below 350 °C while above 400 C crystalline Ta_3N_5 phase due to the lack of enough reducing power for NH_3.[11] While the use of amines and/or NH_3 as reducing agents resulted in cubic TaN XRD peaks at growth temperatures over 400 °C,[13] the thermal ALD from $TaCl_5$ or $TaBr_5$ and NH_3 and TMA produced Ta(Al)N(C) films, which were polycrystalline with cubic TaN XRD peaks for 300 °C or higher temperature.[11] For the current process, polycrystalline cubic TaN films were obtained even for as low temperature as 100 °C.[15] In the previous reports on PE-ALD of TaN by TBTDET, the hydrogen plasma process produced polycrystalline phase while thermal ALD produced amorphous structure.[6] These results

together with previous reports indicate that the plasma enhancement helps the crystallization of the deposited film with high enough reducing power for producing low resistivity polycrystalline TaN. However, it should be noted that our previous report for PE-ALD Ta from $TaCl_5$ and atomic H has shown the amorphous film formation for $TaCl_5$ and atomic H reaction.[5] The exact reason for the difference in microstructure of PE-ALD Ta and TaN is not clear, but we can infer that the presence of activated nitrogen should contribute to the crystallization of the films. In addition, although the TEM study has not been performed for PVD cubic TaN phase in this study, the previous reports have shown that the cubic TaN layer consists of small grains with a few nm size, which is similar to the current PE-ALD TaN thin films.[1,18,20]

The TEM indicates that the surface of PE-ALD TaN is quite smooth. Further measurements on the surface morphology of the deposited film have been done by AFM, with quantative measurements of roughness. Fig. 2 shows the AFM images of the PE-ALD TaN films deposited on SiO_2 for 200 cycles (48Å thick, Fig. 2a) and 1600 cycles (384 Å thick, Fig. 2b). For both thicknesses, RMS roughness did not show significant difference with thickness, 1.5 Å for 200 cycles and 2.1 Å for 1600 cycles, indicating that the PE-ALD TaN has quite smooth surface for up to several hundreds Å thickness. Additionally, the conformality of PE-ALD TaN films have been measured by cross sectional SEM. For the extreme case scenario, very deep trench capacitor structure, with aspect ratio of 60:1 with width of 120 nm was used and over 70 % of step coverage was obtained. For 10:1 aspect ratio of trench structure almost 100 % conformality was obtained. Thus, in terms of roughness and conformality, the application of the current process does not have any problem as Cu diffusion barrier, which is in the thickness range from 5 – 20 nm on lower aspect ratio than 5:1 typically.

The systematic study on the roughness for ALD of metals and nitrides thin films has been rare. One of the common misconceptions for ALD is that the surface morphology would be smooth since the ALD occurs through self-saturation. However, atomically smooth film is not always obtained for ALD. Previous reports have shown that the surfaces of ALD oxides are often quite rough, which was primarily induced by the interface energy between film and substrates and closely related to the surface movement of admolecules.[27] For example, the roughness of TiO_2 ALD film from $TiCl_4$ and H_2O increases with increasing thickness with quite large agglomerations,[28] while Al_2O_3 ALD with similar chemistry has shown very smooth morphology with little increase in RMS value with thickness.[27] For the current TaN PE-ALD process, the surface roughness did not increase significantly with increasing thicknesses up to 1600 cycle of deposition. The one-to-one comparison with PVD counterpart was not performed in terms of roughness, but the previous report on PVD TaN with 15 % nitrogen content has shown that the RMS roughness for 157 nm thickness film was about 17 Å.[29] For PE-CVD of TaN, RMS roughness was 16 Å for 1100 Å thick TaN.[26]

Fig. 3 shows the XRD spectra of the PE-ALD TaN samples on Si substrates after rapid thermal annealing (RTA) up to 1000 °C temperature. For RTA, the samples were heated to the desired temperature with 3 °C/s ramping rate in He environment and stayed at the annealing temperature for 5 secs. Fig. 3a is the reference XRD spectrum for as-deposited PE-ALD TaN films, showing well-distinguished cubic TaN peaks (111 peak at $2\theta = 35.876°$ and 200 peak at $2\theta = 41.638°$). After RTA, no change in the spectra is observed, without showing formation of other phase other than cubic TaN up to 1000 °C of annealing temperatures. (Figs. 3b and c) Similarly, no change in XRD has been observed for PE-ALD TaN on SiO_2 substrates for up to 1000 °C of annealing temperature by RTA.

To obtain further information on the film properties and thermal stability, the samples grown on Si and thin SiO_2 have been analyzed by MEIS. The physics of MEIS is similar to RBS, with the distinctions arising from the ion beam energy and detector technology, so the spectra can be interpreted using the same principles. For ultrathin films, MEIS has the advantages of subnanometer depth resolution and sensitivity to light elements, such as oxygen. Since ions lose energy as they penetrate a film, the energy loss can be directly converted to a depth scale.[30] Fig. 4a shows the typical MEIS spectrum for TaN PE-ALD film deposited on Si surface for 100 cycles. (24 Å thickness) In addition to Ta and nitrogen peaks from the deposited film, Si from substrate was observed. Although Cl peak was not observed indicating the film is quite pure, oxygen peak was clearly seen. To find out the distribution of each component, the MEIS spectrum was simulated based upon the multiplayer structure and the simulated result is shown in the figure. From the comparison between simulation and experimental data, it was found that the oxygen-containing layer resides only at top 10 Å surface. This result indicates that the oxygen in the film is mostly incorporated by post-deposition air exposure. Additional MEIS analysis on 50 cycles PE-ALD TaN on Si thin oxide film has shown that the TaN films were continuous up to 12 Å thickness.

The oxygen contents of ALD transition nitride films have been reported to be high for most cases. In a pervious report on the TiN ALD from $TiCl_4$ and NH_3, the oxygen was suggested to be incorporated by post-deposition air exposure, based upon the observation that the O concentration in the film decreases with thickness (from 32 at.% for 340 Å to 3 at.% for 1400 Å).[31] The oxygen was determined to be evenly distributed through the film from RBS analysis, which was attributed to the diffusion of oxygen through grain boundaries of polycrystalline TiN film. In other report on TiN ALD, however, O content was measured as highest at surface region,

which strongly supports that the O is incorporated by post deposition air exposure.[32] While these previous results were from analysis techniques which do not possess high enough depth resolution, the current MEIS analysis in this work, which has sub nm scale depth resolution, has shown that the oxygen is only in the surface region for TaN PE-ALD. This result supports that the oxygen contamination is by post deposition oxidation and the oxygen redistribution after deposition is much limited for TaN PE-ALD.

The same specimen was annealed inside of the MEIS analysis chamber for 800 to 1000 °C. After each annealing process, MEIS spectra have been obtained. (Fig. 4b) The spectra shows decrease in oxygen peak, especially for 900 and 1000 °C annealing, indicating that the O containing layer is reduced to TaN layer with high temperature vacuum annealing. However, no indication of interaction or intermixing between Si and TaN layer was observed, agreeing with XRD data (Fig. 3). Similar results were obtained for PE-ALD TaN films deposited on thin silicon oxide substrates.

The thermal stability is prerequisite for liner materials as diffusion barrier layer. Among various phases of Ta nitrides, TaN deposited from PVD has been reported to have highest thermal stability with Si substrate. For PVD cubic TaN, no reaction was observed up to 800 - 900 °C of annealing for 30 minutes and nitrogen loss has not been observed by annealing up to 800 °C.[1,19,23] Meanwhile, for the amorphous CVD TaN_x film from $TaBr_5$, no reaction between TaN and Si was observed by thermal annealing up to 650 °C by RBS.[9] But at annealing temperatures above 600 °C, changes in microstructure was observed from amorphous to crystalline phase. The present investigations from XRD and MEIS of PE-ALD TaN films have shown good thermal stability, at least up to 1000 °C, against Si and SiO_2 substrates. All these results including smoothness and good conformality as well as continuity at nm scale observed

by MEIS support that the current PE-ALD TaN films have good structural characteristics as diffusion barrier.

Fig. 5 shows the typical Cu diffusion barrier measurement results using three different analysis techniques for 200 nm PVD Cu/2 nm ALD TaN/poly-Si stack. Fig 5a is the X-ray diffraction intensity contour map for the bilayer sample during an annealing from 100 to 1000 °C at 3 °C/s (only the data from 550 to 800 °C are shown). The X-ray detector is placed such that the Cu(111) and Cu silicide reflections are present in the selected 2θ range (44 to 56°). The intensity is plotted as a function of annealing temperature and lower intensity is shown by darker shading. As is evident from the figure, the Cu(111) peak starts to decrease in intensity around 640 °C as the Cu silicide peak grows in intensity. The Cu silicide peak at 2θ = 52.5° corresponds to the 320 diffraction of η'' Cu_3Si phase.[24] Fig. 5b and 5c shows the normalized elastic light scattering intensity for two different lateral length scale (0.5 and 5 nm) and sheet resistance, which were measured simultaneously, as a function of annealing temperature. The elastic scattering intensities for both length scales start to increase around 620 °C, indicating changes in surface roughness and/or index of refraction due to barrier failure. At the same temperature, the resistance result shows an abrupt increase in sheet resistance, indicating the start of barrier failure. When Cu is deposited right on the HF cleaned Si substrates (i.e., Si without native oxide), Cu silicide formation was observed at about 260 °C. Thus, the thin PE-ALD TaN layer effectively prohibit the diffusion of Cu to the underlying Si substrate.

Fig. 6 shows the synchrotron X ray diffraction contour map for PE-ALD TaN with three different thicknesses, 2.5, 5, and 12.5 nm. The Cu 111 peak disappears at higher temperature with increasing thickness. For example, the Cu 111 peak stays up to above 820 °C, indicating that the Cu diffusion is much more effectively prohibited by thick PE-ALD TaN. For

comparison, the same test structures were prepared by separate DC magnetron PVD chambers for same thicknesses of TaN (2.5, 5, and 12.5 nm). Since the different N content could results in differences in diffusion barrier failure temperatures,[19,20] cautions were taken to obtain stoichiometric nitrogen content during PVD and RBS confirmed the chemical component for the prepared samples. The prepared PVD TaN samples were analyzed by the same techniques, and the Cu diffraction peak disappeared at similar temperatures with PE-ALD TaN at comparable thickness.

The barrier failure temperatures for PE-ALD and PVD TaN layers are represented in Fig. 7. Here, the barrier failure temperature was defined using the disappearance of the Cu 111 peak; by taking the derivatives of the integrated XRD peak intensity versus annealing temperature, the minima obtained were recorded as the barrier failure temperature. The data shows that there is little difference in diffusion barrier failure temperature for ALD and PVD TaN. For comparison purpose, the failure temperatures of PE-ALD and PVD Ta from previous report obtained by the same analysis techniques are shown together.[5] The figure shows that PE-ALD Ta has higher failure temperature for smaller thickness below 8 nm, while lower values for thicker films.

IV. Discussions.

There have been extensive studies on the Ta based diffusion barrier properties for Cu interconnects. It has been shown that the failure of the PVD Ta barrier between Cu and Si is first indicated by η'' Cu_3Si formation at the Ta-Si interface caused by the diffusion of Cu through Ta films, followed by accelerated Ta_5Si_3 and $TaSi_2$ formation.[2,16] The diffusion barrier properties of Ta were improved with impurities such as hydrogen and oxygen in the film.[17] For tantalum nitirides as a diffusion barrier for Cu, cubic TaN phase has been found to have higher failure

temperature compared to Ta_2N layer.[18] This was mainly attributed to the higher thermal stability against Si substrates. For example, the 25 nm thick TaN failed after 800 °C for 30 minutes, while Ta_2N failed at 650 °C.[19] For TaN layer, the formation of Cu silicide is the main failure mechanism after Cu diffusion through TaN layer, similar to Ta case.[18-20] One study on diffusion barrier properties of PVD Ta and TaN as a function of thickness from electrical measurements has shown that the failure temperature changes from 550 to 450 °C as thickness decreases from 25 to 5 nm for Ta and 700 to 500 C for TaN.[23]

So far, most of the reports on diffusion barrier properties of CVD or ALD TaN layers have been on high nitrogen phase or TaN with high impurities. For the ALD of cubic Ta(Al)N(C) film, deposited from $TaCl_5$, NH_3, and TMA, the failure temperature was found to be around 600 °C by XRD for 10 nm thick film.[11] For nitrogen rich TaN_x layer by thermal CVD either from halide ($TaBr_5$) or MO (TBTDET) precursors, lower Cu diffusion barrier failure temperatures were obtained compared to PVD TaN_x.[9,10,21] The poorer performance of CVD TaN_x was explained by the amorphous to crystalline phase (Ta_3N_5) transition,[9] or more dense structure of PVD TaN films with different preferred orientation[21]. Meanwhile, for the ion beam induced CVD TaN_x from PDEAT, the resistivity and oxygen content was lower and the diffusion barrier failure temperature was higher than thermal process.[10,22] The better performance of ion beam induced CVD TaN_x as diffusion barrier was attributed to the higher density.

In the present study, we have estimated the failure temperatures for Cu diffusion barrier of low resistivity cubic TaN deposited by PE-ALD. The failure temperatures were obtained by continuous ramping of the sample temperature. By this, fast determination of the failure temperatures was possible, with the support of other in situ analysis techniques. However, since the most of the previous studies have employed steady state annealing (ie, annealing at a constant

temperature for a certain amount of time, typically 30 to 60 minutes), the resulting diffusion barrier failure temperature should be different. To address this issue, we have used simple quantitative analysis. The average diffusion length (L) can be calculated by

$$L = 2\sqrt{Dt}\,, \tag{1}$$

where D is the diffusion coefficient and t is the total time.[33] For the steady state annealing, L is calculated from the equation (1), if the diffusion coefficient at that temperature is know. For our measurement condition, however, it is more complicated sine the D is changing as a function of temperature during ramping, and the annealing temperature is also a function of measurement time t. D can be represented by

$$D = D_o \exp\left(-\frac{E_a}{kT}\right), \tag{2}$$

where D_o is pre-exponential factor and E_a is the activation energy and the temperature T is given by,

$$T = T_o + rt \tag{3}$$

where T_o is the initial temperature of the measurements (100 °C for present study) and r is the ramping rate (3 °C/s for the current study). Thus, by combining equation (1) – (3) the diffusion length was calculated numerically as a function of annealing temperature. The comparison between the diffusion length calculated from steady state annealing and ramping experiments are shown in Fig. 8. For this calculation, we have used the previously reported diffusion coefficient for Cu in TaN ($D_o = 8.7\text{x}10^{-4}$ cm^2s^{-1}, $E_a = 2.7$ eV).[19] In this example, the diffusion lengths for 30 minutes of diffusion time are shown for steady state annealing (solid line), and diffusion lengths for ramping annealing (dotted line) are shown as a function of the final temperature of the ramping, which started at 100 °C with ramping rate of 3 °C/s (current measurement condition). As expected, the diffusion length for steady state annealing is longer than the

ramping annealing, since the total time of annealing is shorter (for the final temperature of 1000 °C, the total time of annealing is 5 minutes for example) and the average diffusion coefficient is smaller for ramping annealing. (11.4 Å for ramping and 21.4 Å for steady state annealing at 600 °C)

If the diffusion length can be thought as a diffusion barrier layer thickness, the temperature in Fig. 8 corresponds to the failure temperature. Thus, this implies that for the same thickness of barrier, the current experimental condition would result in several tens of degree higher failure temperature. The same calculated curve (dotted line) is replotted in Fig. 9, now represented as the failure temperature as a function of barrier thickness. For comparison, the experimental data of PE-ALD TaN and PVD TaN (shown in Fig. 7) are shown together. The experimental data agree reasonably for 12.5 nm thick, but deviate to lower temperature with the thickness decrease. We attribute this to the grain boundary diffusion of Cu. It is well know that the grain boundary is "high diffusion path" and the activation energy for grain boundary is almost half of that of diffusion in lattice.[33] Thus, the diffusion coefficient in polycrystalline is higher than in single crystal at lower temperature. For example, self diffusion coefficients of Ag for single crystal and polycrystalline Ag have same value above 700 °C, while that for polycrystalline Ag has higher value below this temperature. Similar behavior has been observed for Cu diffusion through TaN barrier.[19] Oku et al estimated the diffusion coefficient of Cu in TaN as a function of annealing temperature based upon the time to failure at different annealing temperatures from XRD.[19] The activation energy of Cu diffusion in TaN was estimated as 2.7 eV for above 800 C, while it was 1.3 eV below 800 °C. From this, the lattice diffusion coefficient of Cu in TaN (D_l) was estimated as $D_l = 8.7\text{x}10^{-4}\exp(-2.7\ \text{eV/kT})$, while the grain boundary diffusion coefficient (D_{gb}) as $2.8\text{x}10^{-10}\exp(-1.3\ \text{eV/kT})\ \text{cm}^2\text{s}^{-1}$. According to this, we

have recalculated the diffusion length as a function of annealing temperature (ie. failure temperature vs. barrier thickness) using the D value of $2.8x10^{-10}exp(-1.3\ eV/kT)\ cm^2s^{-1}$ below 800 °C. The calculated results are plotted in Fig. 9 as a solid line. The experimental data agrees very well with the calculations.

Considering the difference in preparation of the samples and measurement techniques between current study and ref. 19, the agreement is quite impressive. One thing to be noticed here is that the determination of the failure temperature from both the current study and ref 19 was based upon the same analysis techniques, XRD. If analysis techniques with different sensitivity have been used, the comparison would be difficult. For example, the etch pit test or electrical measurements would have produced lower failure temperatures. Other point is that the grain boundary effects are much more clearly seen at smaller thickness. For example, the calculated failure temperature difference is over 100 °C at 20 Å, while it is only 25 °C at 200 Å. Thus, the grain boundary effects become more important as the thickness of diffusion barrier becomes thinner. Due to the grain boundary diffusion, the failure temperature at ultra-thin diffusion barrier becomes more rapidly decreased with thickness decrease for polycrystalline diffusion barrier.

The very good thermal stability of PE-ALD TaN layer supports the previous reports of Cu diffusion barrier failure mechanism; the diffusion barrier failure of polycrystalline TaN occurs by the Cu diffusion through TaN layer, rather than caused by interaction between TaN and Si substrate. The diffusion barrier property measurements in this study indicate that the microstructure may be the one of the most important factors determining the failure, if the Cu diffusion barrier failure mechanism is same. This is supported by the failure temperature data showing that little difference has been observed as a function of thickness for PE-ALD and PVD

TaN. While the ALD TaN has higher Cl content, the failure temperature with thickness show same trend with PVD, indicating Cl content is not important factor. For Ta and TaN, the failure mechanism is known to be similar, mainly determined by Cu diffusion through diffusion barrier. At large thickness, where the bulk diffusion contributes more, the TaN has much better failure temperature than Ta for ALD and PVD alike. This is probably because the lattice diffusion coefficient of Cu in Ta is smaller than in TaN. However, for very thin layer, where the grain boundary play more important role, the ALD Ta has best performance. Due to the amorphous structure, there is no high diffusivity path for Cu through PE-ALD Ta, so the diffusion failure temperature remains high even for very thin layer. Moreover, for very small thickness of 2 nm, the ALD Ta, PVD TaN, ALD TaN films, which all have polycrystalline structure, show similar diffusion barrier failure temperatures. This indicates that the Cu diffusion through grain boundary solely determines the failure temperature for very thin diffusion barriers. All these results indicate that as the diffusion barrier thickness becomes thinner with the downscaling of the devices, the control of film microstructure becomes more important.

V. Conclusions.

The physical properties of PE-ALD TaN as Cu diffusion barrier were investigated. The microstructure, conformality, surface smoothness, and chemical composition analysis all have shown that the current PE-ALD TaN process produces proper diffusion barrier material. The failure temperatures of TaN films as Cu diffusion barriers were estimated from synchrotron XRD, optical scattering, and resistivity measurements and the results were comparable to those of PVD counterpart. From the simple diffusion length calculation and comparison with

amorphous PE-ALD Ta, it has been shown that the microstructure and grain boundary diffusion is the main factor to determine diffusion barrier failure for Cu interconnect.

Acknowledgments

The authors gratefully acknowledge IBM colleagues including Andrew Kellock, and Dae-Gyu Park for their helps on analysis of samples.

.

References

1. X. Sun, E. Kolawa, J.-S. Chen, J.S. Reid, and M.-A. Nicolet, Thin Solid Films, **236**, 347 (1993).
2. K. Holloway, P.M. Fryer, C. Cabral Jr., J.M.E. Harper, P.J. Bailey, and K.H. Kelleher, J. Appl. Phys. **71**, 5433 (1992).
3. M. Lane, R. H. Dauskardt, N. Krishna, and I. Hashim, J. Mater. Res. **15**, 203 (2000).
4. S.M. Rossnagel and H. Kim, Proceedings of the IEEE 2001 International Interconnect Technology Conference, p3 (2001).
5. H. Kim, C. Cabral, Jr., C. Lavoie, and S.M. Rossnagel, J. Vac. Sci. Technol. **B20**, 1321 (2002).
6. J.-S. Park, H.-S. Park, and S.-W. Kang, J. Electrochem. Soc. **149**, C28 (2002).
7. N. Terao, Jpn. J. Appl. Phys. **10**, 248 (1971).
8. C.-S. Shin, Y.W. Kim, D. Gall, J.E. Greene, and I. Petrov, Thin Solid Films **402**, 172 (2002).
9. A. Kaloyeros, X. Chen, T. Stark, K. Kumar, S.-C. Seo, G.G. Peterson, H.L. Frisch, B. Arkles, and J. Sullivan, J. Electrochem. Soc. **146**, 170 (1999).
10. S.-L. Cho, K.-B. Kim, S.-H. Min, H.-K. Shin, and S.-D. Kim, J. Electrochem Soc. **146**, 3724 (1999).
11. M. Ritala, P. Kalsi, D. Riihelä, K. Kukli, M. Leskelä, and J. Jokinen, Chem. Mater. **11**, 1712 (1999).
12. P. Alén, M. Juppo, M. Ritala, T. Sajavaara, J. Keinonen, and M. Leskelä, J. Electrochem. Soc. **148**, G566 (2001).

13. P. Alén, M. Juppo, M. Ritala, M. Leskelä, T. Sajavaara, and J. Keinonen, J. Mater. Res. **17**, 107 (2002).
14. M. Juppo, M. Ritala, and M. Leskela, J. Electrochem. Soc. **147**, 337 (2000).
15. H. Kim, A.J. Kellock, and S.M. Rossnagel, J. Appl. Phys. **92**, 7080 (2002).
16. T. Laurila, K. Zeng, J.K. Kivilahti, J. Molarius, and I. Suni, Thin Solid Films **373**, 64 (2000).
17. L.A. Clevenger, N.A. Bojarczuk, K. Holloway, J.M.E. Harper, C. Cabral Jr., R.G. Shad, F. Cardone, and L. Solt, J. Appl. Phys. **73**, 300 (1993).
18. K.-H. Min, K.-C. Chun, and K.-B. Kim, J. Vac. Sci. Technol. **B14**, 3263 (1996).
19. T. Oku, E. Kawakami, M. Uekubo, K. Takahiro, S. Yamaguchi, and M. Murakami, Appl. Surf. Sci. **99**, 265 (2996).
20. M. Takeyama, A. Noya, T. Sase, and A. Ohta, J. Vac. Sci. technol. **B14**, 674 (1996).
21. M.H. Tsai, S.C. Sun, C.E. Tsai, S.H. Chuang, and H.T. Chiu, J. Appl. Phys. **79**, 6932 (1996).
22. S.-J. Im, S.-H. Kim, K.-C. Park, S.-L. Cho, and K.-B. Kim, Mat. Res. Soc. Symp. Proc. **612**, D6.7.1. (2000).
23. M.T. Wang, Y.C. Lin, and M.C. Chen, J. Electrochem. Soc. **145**, 2538 (1998).
24. C. Cabral Jr., C. Lavoie, J.M.E. Harper, and J. Jordan-Sweet, Thin Solid Films, **397**, 194 (2001).
25. J. Uhm and H. Jeon, Jpn. J. Appl. Phys. **40**, 4657 (2001).
26. X. Chen, H.L. Frisch, A.E. Kaloyeros, B. Arkles, and J. Sullivan, J. Vac. Sci. technol. **B17**, 182 (1999).
27. M. Ritala, H. Saloniemi, M. Leskelä, T. Prohaska, G. Friedbacher, and M. Grassbauer, Thin Solid Films **286**, 54 (1996).

28. M. Ritala, M. Leskela, L.-S. Johansson, and L. Niinisto, Thin Solid Films **228**, 32 (1993).
29. T. Riekkinen, J. Molarius, T. Laurila, A. Nurmela, I. Suni, and J.K. Kivilahti, Microelectronic Engineering **64**, 289 (2002).
30. M. Copel, E. Cartier, and F.M. Ross, Appl. Phys. Lett. **78**, 1607 (2001).
31. M. Ritala, M. Leskelä, E. Rauhala, and P. Haussalo, J. Electrochem. Soc. **142**, 2731 (1995).
32. C.H. Ahn, S.G. Cho, H.J. Lee, K.H. Park, and S.H. Jeong, Metals and materials International **7**, 621 (2001).
33. P. Shewmon, "Diffusion in Solids", 2nd ed. The Minerals, Metals, and Materials Society. 1989.

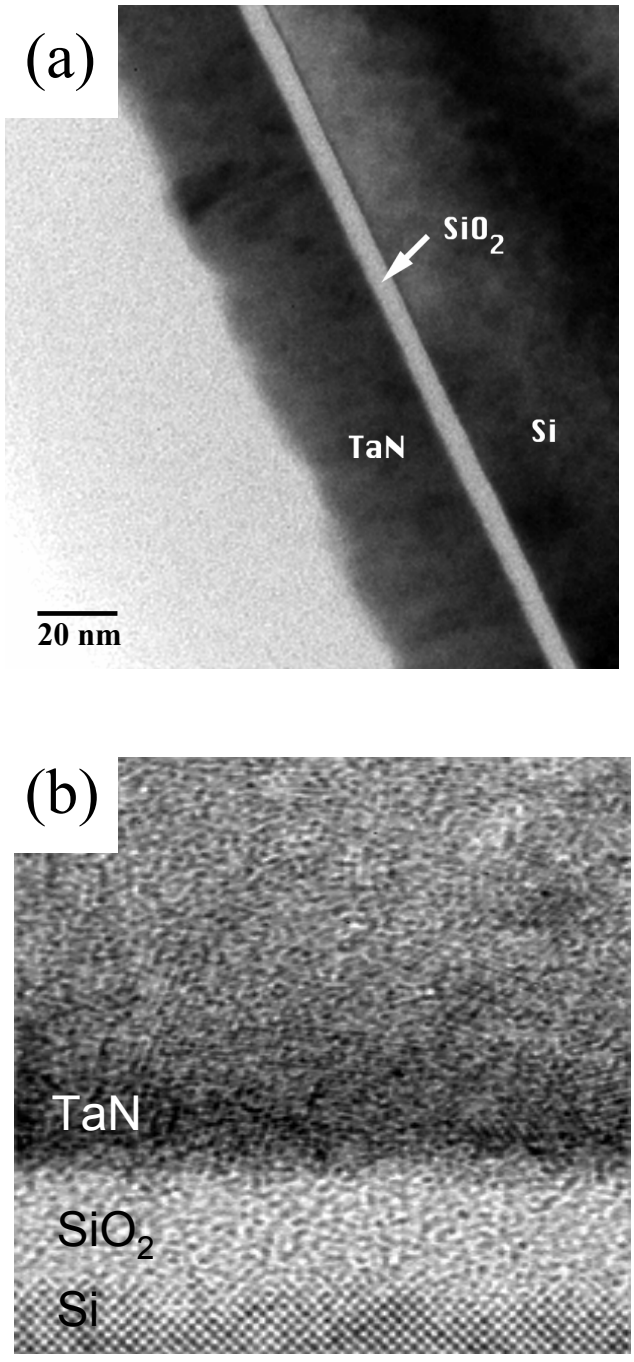

Fig. 1. (a) The cross sectional TEM image for TaN PE-ALD films deposited on SiO_2 substrate and (b) the high resolution image. The growth temperatures were 300 °C.

(a) 200 cycles

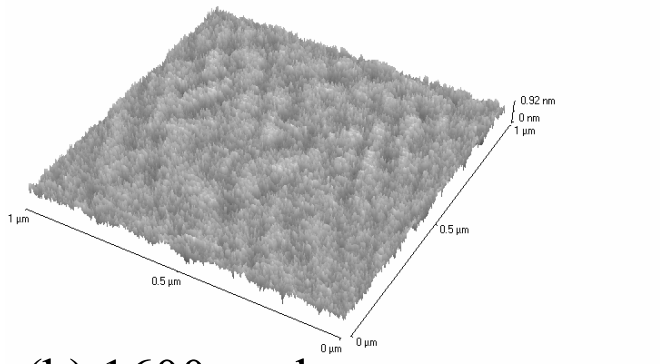

(b) 1600 cycles

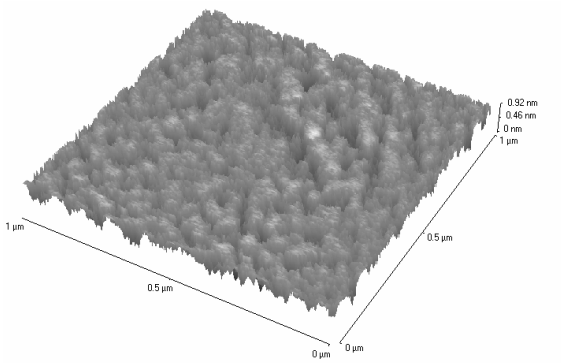

Fig. 2. The AFM image of PE-ALD TaN grown at 300 °C on SiO_2 surface, for (a) 200 cycles and (b) 1600 cycles.

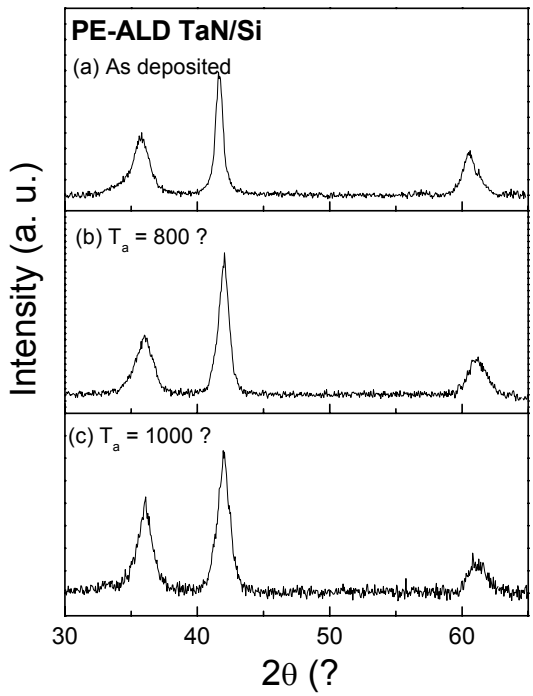

Fig. 3. XRD spectra of PE-ALD TaN on Si substrates for (a) as-deposited, (b) annealed at 800 °C, and (c) 1000 °C for 30 seconds at RTA chamber in N_2 environment.

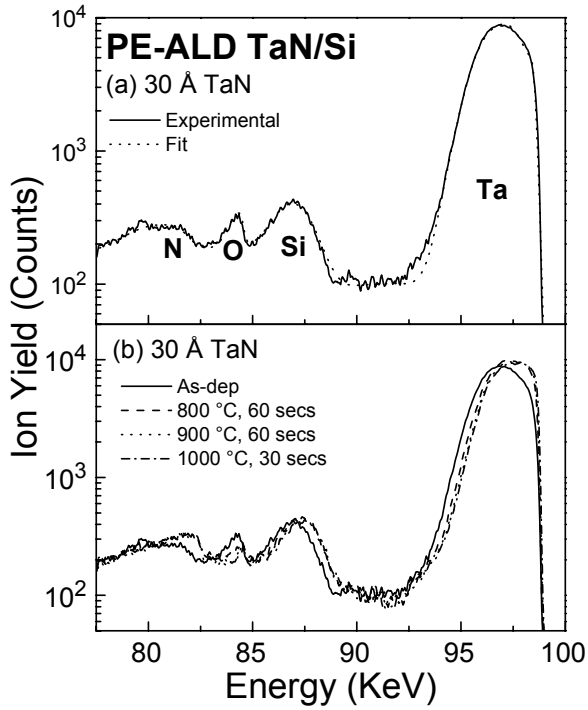

Fig. 4. (a) The MEIS spectrum of PE-ALD TaN films deposited on Si substrate at 300 °C. The thickness was 30 Å and the experimental data are shown as solid line with simulated result as dotted line. (b) The MEIS spectra of PE-ALD TaN films annealed at 800, 900, for 60 seconds and 1000 °C for 30

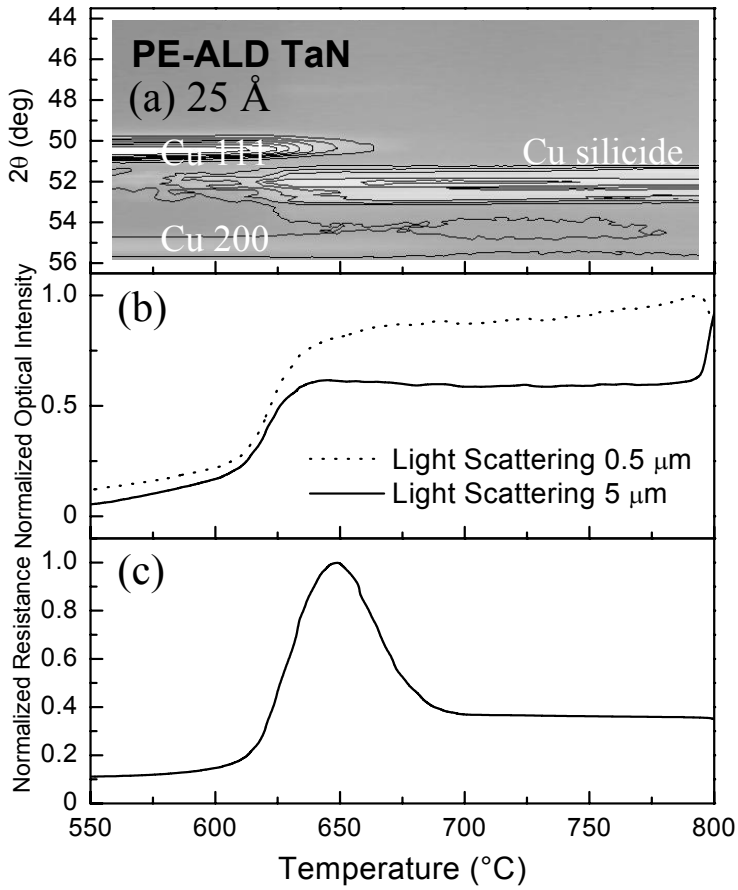

Fig. 5. (a) *In situ* synchrotron X-ray diffraction analysis, (b) optical scattering at two different length scales (0.5 and 5 μm), and (c) resistance analysis as a function of annealing temperature for 200 nm PVD Cu/2.5 nm ALD TaN/poly-Si structure. The sample was annealed at 3 °C/s from 100 to 1000 °C in forming gas and all three analyses were performed simultaneously.

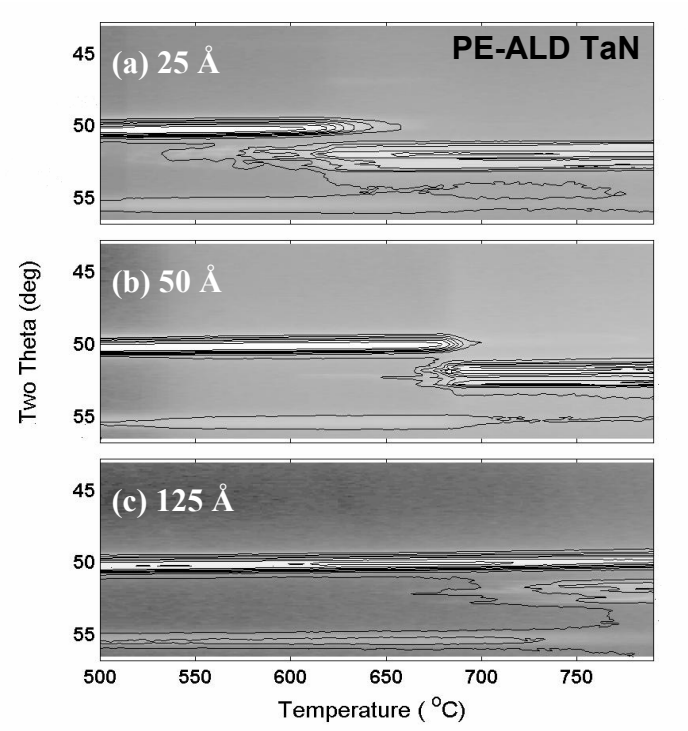

Fig. 6. *In situ* synchrotron X-Ray diffraction analysis as a function of annealing temperature for (a) 200 nm PVD Cu/2.5 nm ALD Ta/poly-Si, (b) 200 nm PVD Cu/5 nm PVD Ta/poly-Si, and (c) 200 nm PVD Cu/12.5 nm ALD Ta/poly-Si. The samples were annealed at 3 °C/s from 100 to 1000 °C in forming gas.

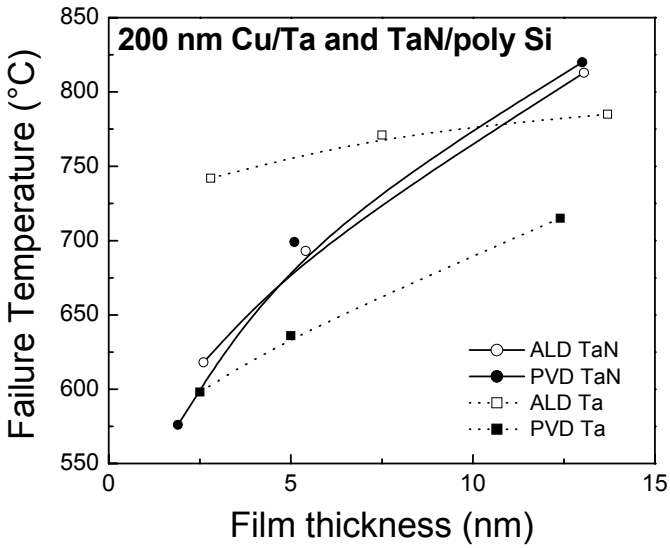

Fig. 7. Barrier failure temperatures determined using in situ X-ray diffraction analysis comparing ALD and PVD Ta and TaN diffusion barriers grown on poly-Si substrates.

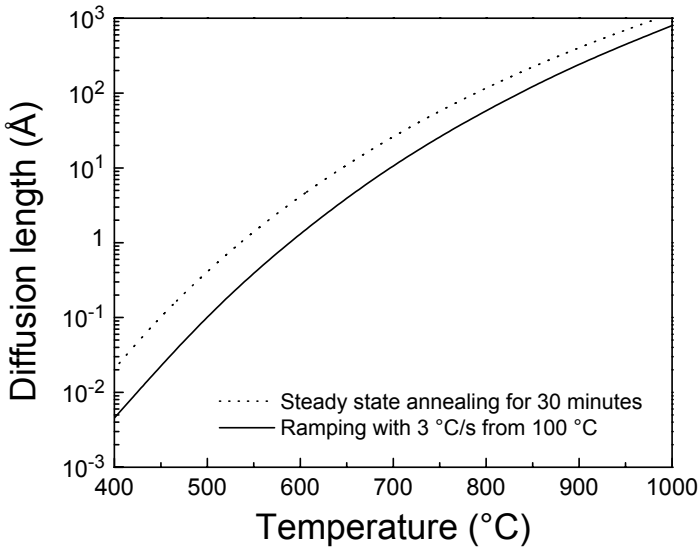

Fig. 8. Calculated diffusion length using the simple diffusion length equation for steady state annealing for 30 minutes (solid line) and annealing with ramping rate 3 °C from 100 °C to the given temperature (dotted line). The Cu diffusion barrier coefficient in TaN lattice has been used.(19)

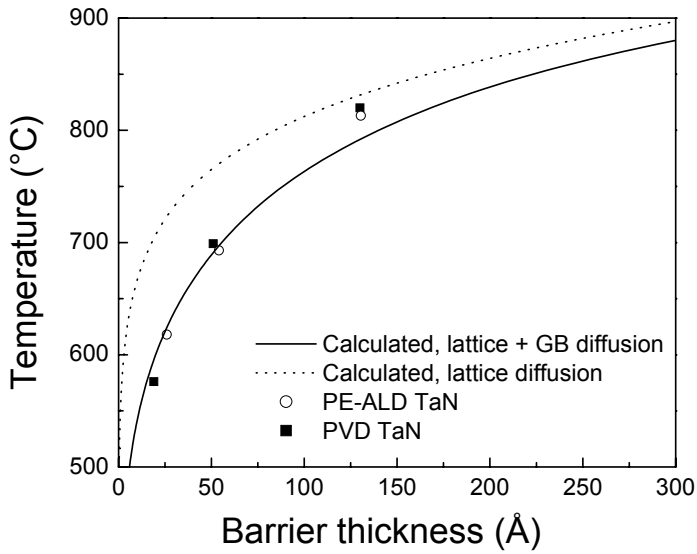

Fig. 9. Calculated diffusion length based upon the diffusion coefficient reported on ref. 19. The dotted line is for lattice diffusion only while solid line is considering grain boundary diffusion together. For comparison, the failure temperature for PVD and PE-ALD TaN are shown together.